



**HAL**  
open science

## Photochemical modeling of Titan atmosphere at the "10 percent uncertainty horizon"

Zhe Peng, M. Dobrijevic, Eric Hébrard, Nathalie Carrasco, Pascal Pernot

### ► To cite this version:

Zhe Peng, M. Dobrijevic, Eric Hébrard, Nathalie Carrasco, Pascal Pernot. Photochemical modeling of Titan atmosphere at the "10 percent uncertainty horizon". *Faraday Discussions*, 2010, 147, pp.137-153. 10.1039/c003366a . hal-00509656

**HAL Id: hal-00509656**

**<https://hal.science/hal-00509656>**

Submitted on 28 Sep 2022

**HAL** is a multi-disciplinary open access archive for the deposit and dissemination of scientific research documents, whether they are published or not. The documents may come from teaching and research institutions in France or abroad, or from public or private research centers.

L'archive ouverte pluridisciplinaire **HAL**, est destinée au dépôt et à la diffusion de documents scientifiques de niveau recherche, publiés ou non, émanant des établissements d'enseignement et de recherche français ou étrangers, des laboratoires publics ou privés.

# Photochemical modeling of Titan atmosphere at the "10 percent uncertainty horizon"

Zhe Peng<sup>a</sup>, Michel Dobrijevic<sup>b</sup>, Eric Hébrard<sup>b</sup>,  
Nathalie Carrasco<sup>c</sup> and Pascal Pernot<sup>a\*</sup>

<sup>a</sup>Laboratoire de Chimie Physique, UMR 8000,  
CNRS, Université Paris-Sud 11, 91405 Orsay cedex, France.

<sup>b</sup> Université de Bordeaux, Laboratoire d'Astrophysique de Bordeaux,  
CNRS/INSU, UMR 5804, BP 89, 33271 Floirac Cedex, France.

<sup>c</sup>Laboratoire Atmosphères, Milieux, Observations Spatiales,  
Université de Versailles Saint-Quentin, UMR 8190,  
91371 Verrières le Buisson cedex, France.

\*Email: pascal.pernot@lcp.u-psud.fr

## Abstract

Titan's atmospheric chemistry modeling is presently limited by the lack of knowledge about many reaction rate coefficients at low temperature (50-200 K). Considering the difficulty of measuring such data, the only way to improve this situation is to identify key reactions as the ones for which better estimations of reaction rates is guaranteed to have a strong influence on the precision of model predictions. This is a slow iterative process, the limit of which has never been clearly defined in terms of model precision. The fact is that this limit is not a fully deterministic simulation, since one should not expect all reaction rate coefficients ever to become available with null uncertainty. The present study considers a quite optimistic scenario, in which reaction rate coefficients in the chemical model are assumed to be known with a 10 % relative uncertainty. The implications for chemical growth modeling are discussed.

# 1 Introduction

The overall precision of photochemical models of planetary atmospheres has unambiguously been shown to be highly sensitive to the uncertainty in the rates of involved chemical reactions.<sup>1-8</sup> Monte Carlo uncertainty propagation enabled Hébrard *et al.*<sup>9</sup> to assess the effect of these uncertainties on the computed abundances of major chemical species predicted by a 1D photochemical model of Titan’s atmosphere. Strikingly, the uncertainties of most of the computed abundances could be much larger than the estimated uncertainty of the abundances gathered from observations, even for basic hydrocarbons like CH<sub>4</sub>, C<sub>2</sub>H<sub>2</sub>, C<sub>2</sub>H<sub>4</sub> and C<sub>2</sub>H<sub>6</sub>.

A major obstacle to precise prediction is the lack of data on the reactivity of neutral species at low temperature (low-T); for instance, in state-of-the-art photochemical models of Titan’s atmosphere, less than 10 % of the reaction rates have been measured in the relevant temperature range. In consequence, photochemical models of Titan’s atmosphere are based mostly on low-T extrapolations of Arrhenius-type laws, which are known to be often inappropriate in this context.<sup>10,11</sup> Until reliable extrapolation models are made available, low-T extrapolation of reaction rates is to be treated with great care and considered as highly uncertain.<sup>12</sup>

Sensitivity analysis can be used to identify *key reactions*, responsible for large uncertainties in model prediction of some target property.<sup>13</sup> This approach guarantees that the reduction of the uncertainty on the rates of key reactions will have the strongest impact on the precision of the target property. This is particularly important to assist in designing new rate constant measurement campaigns or in prioritizing the review by experts of existing data.

The improvement of model precision by key reaction identification/reevaluation is an iterative process (new key reactions are eventually revealed following an update of the previous ones<sup>12</sup>), which can take a very long time to achieve a prescribed precision level. The goal of the present paper is to extrapolate this process and observe what could be expected in the limit where all reaction rates are well determined. We want to emphasize here that an absolute accuracy of reaction rates will probably never be achieved, and we retained here a very optimistic limit of 10 % relative uncertainty for all known reaction rates. Model improvement might also come from the addition of missing processes when they are discovered. Although model complexity is a salient issue in the present study, prediction of model completion effect is beyond the scope of this paper.

Monte Carlo uncertainty propagation was performed for 0D and 1D photochemical models of Titan’s atmosphere and we present here the results and their analysis in order to better understand uncertainty patterns in chemical networks with regard to molecular complexification.

# 2 Methods

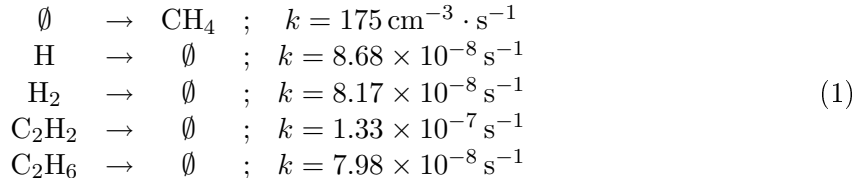
The results of this article are based on three types of chemical models. A 1D photochemical model is used to study the global uncertainty patterns appearing in a complex network, whereas a simpler 0D model, without transport, is better fit to study local uncertainty (at the species level). Elementary models based on simplified reaction networks, are introduced in the course of the analysis to illustrate various observations.

## 2.1 1D and 0D photochemical models

The main lines of the 1D photochemical model and statistical procedures for uncertainty propagation and sensitivity analysis are presented here. More details can be found in Hébrard *et al.*<sup>9</sup> and Dobrijevic *et al.*<sup>13,14</sup>

In our 1D photochemical model extending from Titan’s surface to 1300 km, the species densities are governed by the altitude-dependent continuity-diffusion equation. A detailed description of hydrocarbon, nitriles and oxygen coupled photochemistry, vertical eddy diffusion, molecular diffusion, and radiative transfer (including Rayleigh scattering by N<sub>2</sub> and aerosols absorption) are included in this model. Ions are not considered, and the loss and productions are due to photodissociations, bimolecular and termolecular reactions between neutral species. The model calculates abundances for 127 hydrocarbons, nitriles and oxygenated species, involved in 676 chemical reactions and 69 photodissociation processes.

A preliminary study is based on a simplified 0D model of Titan’s hydrocarbon chemistry at 800 km, proposed by Dobrijevic *et al.*<sup>13</sup> as a benchmark for sensitivity analysis methods. This model contains reactions between H, H<sub>2</sub> and hydrocarbons with less than three carbon atoms, *i.e.* 15 species involved in 48 reactions. This 0D model had no stationary state in Dobrijevic *et al.*<sup>13</sup> and has been completed in the present study with additional production and loss processes, tuned to provide stationary densities close to those of the original model at the representative time  $t = 10^7$ s



Those rates have no attached uncertainty.

## 2.2 Elementary models

To analyze the results of uncertainty propagation in more complex networks, we introduce in the course of this paper a set of basic chemical networks, presented as "Elementary Models" or EMs. For each elementary model (see *e.g.* EM 1), we provide expressions for the stationary state concentration of species of interest  $a_i = [A_i]_{t=\infty}$  and the relative variance  $\sigma_{a_i}^2/a_i^2$ , obtained by the standard law of uncertainty propagation by combination of variances.<sup>15</sup> The corresponding uncertainty factor is  $F_{a_i} = 1 + \sqrt{\sigma_{a_i}^2/a_i^2}$ .

## 2.3 Uncertainty propagation and sensitivity analysis

Vertical structure, solar irradiance and diffusion coefficients (eddy and molecular) were kept fixed throughout the calculations. Uncertain values of photodissociation and reaction rates are represented by lognormal probability distributions

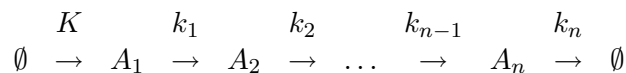
$$p(x) = \frac{1}{\sqrt{2\pi}x\sigma} \exp\left(-\frac{(\ln x - \mu)^2}{\sigma^2}\right) \tag{2}$$

with two parameters  $\mu = \ln k(T)$ , the logarithm of the nominal value of the reaction rate at temperature  $T$ , and  $\sigma = \ln F(T)$ , where  $F(T)$  is the geometric standard uncertainty of the

---

**Elementary Model 1** Linear chain of (quasi-)unimolecular reactions

---

**Scheme****Stationary state concentration**

$$a_i = \frac{K}{k_i}$$

**Relative variance**

$$\frac{\sigma_{a_i}^2}{a_i^2} = \frac{\sigma_K^2}{K^2} + \frac{\sigma_{k_i}^2}{k_i^2}$$

**Notes**

There is no uncertainty accumulation along the chain. The uncertainty of a given species depends only on the initial production rate  $K$  and the loss rate of this species  $k_i$ . The intermediate steps have no influence on the relative uncertainty of species  $i$ . This offers an important simplification rule in the analysis of more complex networks. Note also that if such chains occur in a photochemical model, the photolysis rates (corresponding to  $K$ ) will systematically appear as key reactions.

---

lognormal distribution. With these notations, the 67% confidence interval for a reaction rate at a given temperature is  $[k(T)/F(T), k(T) \times F(T)]$ . For small uncertainties, one can write  $F \simeq 1 + \frac{\Delta k}{k}$ : for instance, a 10% relative uncertainty on  $k$  corresponds to  $F = 1.1$ . The reaction rate coefficients and the photodissociation coefficients used in the present study were extracted from the review by Hébrard *et al.*,<sup>16</sup> with some important revisions detailed in a recent article,<sup>12</sup> but a global uncertainty factor  $F = 1.1$  was assumed for all processes.

For Monte Carlo uncertainty propagation, random reactions rates are generated from their pdf and model outputs are computed for each draw. For the 1D model, long computation times required to reach the stationarity of the species densities limit the number of Monte Carlo samples: typically about 500 independent samples are generated. This provides a convergence of average values and correlation coefficients to better than 5%. For the smaller 0D model, the number of Monte Carlo runs is not limited, and we are able to estimate output uncertainty factors with better than 1% accuracy (10 000 runs).

For each run, one records the reaction rate coefficients (inputs) and neutral mole fractions (outputs) at different altitudes, which are used for statistical uncertainty and sensitivity analysis. Input-output correlation coefficients provide sensitivity measures well adapted to key reaction search.<sup>13</sup> They are easy to estimate within the Monte Carlo uncertainty propagation framework and do not require dedicated sampling schemes.<sup>17,18</sup> The input and output samples recorded for uncertainty evaluation can be directly used for the sensitivity analysis.<sup>12-14,19</sup>

Species	0D model				1D model
	Density (cm <sup>-3</sup> )	$F$ (simul)	$F$ (EM)	EM #	$F$ (simul)
H	$2.6 \times 10^9$	1.03	1.03	2	1.06
H <sub>2</sub>	$1.7 \times 10^9$	1.03	1.03	2	1.03
CH	$2.3 \times 10^2$	1.13	1.12	2	1.11
<sup>3</sup> CH <sub>2</sub>	$2.6 \times 10^1$	1.13	1.14	3	1.08
<sup>1</sup> CH <sub>2</sub>	$9.2 \times 10^1$	1.08	1.09	2	1.11
CH <sub>3</sub>	$4.4 \times 10^7$	1.08	-	-	1.11
CH <sub>4</sub>	$2.2 \times 10^9$	1.07	1.06	2	1.02
C <sub>2</sub> H	$6.0 \times 10^3$	1.24	-	-	1.08
C <sub>2</sub> H <sub>2</sub>	$6.3 \times 10^8$	1.01	1.03	2	1.05
C <sub>2</sub> H <sub>4</sub>	$2.4 \times 10^8$	1.07	1.07	2	1.05
C <sub>2</sub> H <sub>5</sub>	$2.6 \times 10^1$	1.20	-	-	1.13
C <sub>2</sub> H <sub>6</sub>	$4.1 \times 10^7$	1.31	-	-	1.09

Table 1: Densities and uncertainty factors for all species of the 0D model. Simulation results for uncertainty factors,  $F$ (simul), are compared to estimations by Elementary Models,  $F$ (EM), when available. The last column reports uncertainty factors for the same species as simulated with the 1D model at 900 km. All simulations are run with a uniform uncertainty factor  $F = 1.1$  on reaction rate constants.

### 3 Results and discussion

#### 3.1 Analysis of the 0D simulations

Stationary densities and the associated uncertainty factors are given in Table 1. We observe that many species densities are simulated with uncertainty factors smaller than  $F = 1.1$ , as low as  $F = 1.01$  for C<sub>2</sub>H<sub>2</sub> or  $F = 1.03$  for H and H<sub>2</sub>. By contrast, two species have remarkably enhanced uncertainty factors: C<sub>2</sub>H ( $F = 1.24$ ) and C<sub>2</sub>H<sub>6</sub> ( $F = 1.31$ ).

We will show now how these observations can be interpreted through elementary models, mostly based on unimolecular or pseudo-unimolecular reactions.

##### 3.1.1 C<sub>2</sub>H<sub>4</sub>, H<sub>2</sub>, H, CH<sub>4</sub>, CH and <sup>1</sup>CH<sub>2</sub>

These species have an uncertainty factor smaller than the nominal value ( $F = 1.1$ ) and are affected by numerous production and/or loss processes. For instance, C<sub>2</sub>H<sub>4</sub> has 12 production pathways and 2 loss reactions. This pattern can be linked to EM 2, in the hypothesis of independent pathways. Observing that in this case all pathways have almost equivalent contributions, we have

$$F_{C_2H_4} = 1 + \sqrt{\left(\frac{1}{12} + \frac{1}{2}\right) \times 0.1^2} \quad (3)$$

$$\simeq 1.08 \quad (4)$$

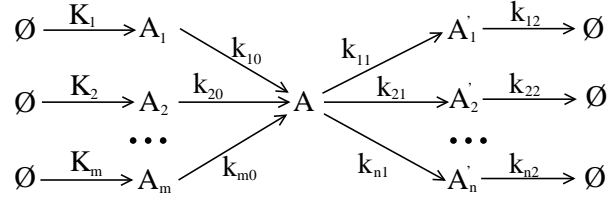
which is very close to the value obtained by simulation ( $F = 1.07$ ). When pathways have different contributions, we use the general expression for EM 2, which provides also favorable comparisons for H<sub>2</sub>, H, CH<sub>4</sub>, CH and <sup>1</sup>CH<sub>2</sub> (see Table (1)), validating the initial hypothesis of pathways independence. Indeed, almost all species densities in this model are correlated

---

**Elementary Model 2**  $m$  productions -  $n$  losses
 

---

Scheme



Stationary state concentration

$$a = \frac{\sum_{i=1}^m K_i}{\sum_{i=1}^n k_{i1}}$$

Relative variance

$$\frac{\sigma_a^2}{a^2} = \sum_{i=1}^m \left( \frac{K_i}{\sum_{j=1}^m K_j} \right)^2 \frac{\sigma_{K_i}^2}{K_i^2} + \sum_{i=1}^n \left( \frac{k_{i1}}{\sum_{j=1}^n k_{j1}} \right)^2 \frac{\sigma_{k_{i1}}^2}{k_{i1}^2}$$

Notes

- The results are independent on the rates  $k_{i0}$  of direct production processes of  $A$ .
- In the case of equal values of  $\{K_i\}$  and  $\{k_{j1}\}$ , one gets

$$\frac{\sigma_a^2}{a^2} = \frac{1}{m} \frac{\sigma_{K_i}^2}{K_i^2} + \frac{1}{n} \frac{\sigma_{k_{j1}}^2}{k_{j1}^2}$$

The production and loss contributions are independent, and in both cases, the relative variance is inversely proportional to the number of processes, which follows from the standard law for the sum of independent random variables.

---

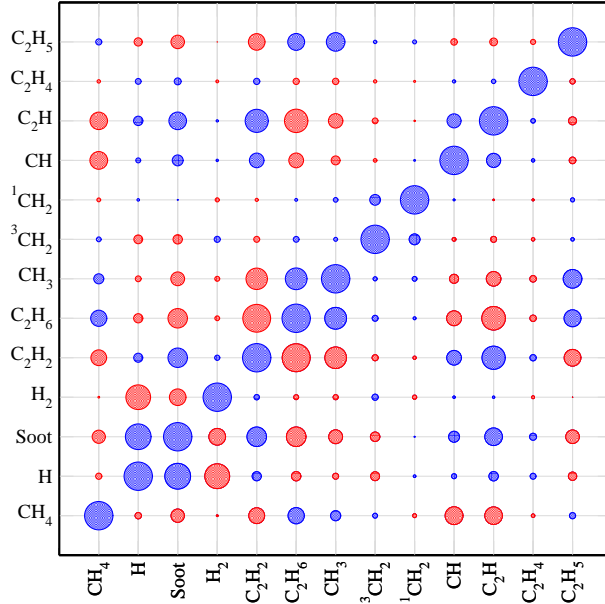


Figure 1: Correlation matrix between stationary densities of species in the 0D model: (blue) positive correlation; (red) negative correlation. Linear scale of symbol size from 1 (on the diagonal) to 0.

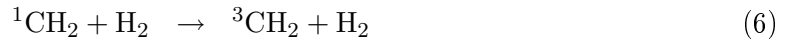
by reactions, but we observe that, due to this general correlation, individual correlations are typically weak, even in the case where two species are directly linked by a bimolecular reaction (Fig. (1)).

### 3.1.2 $^3\text{CH}_2$

This species has an uncertainty factor  $F = 1.13$ , larger than the nominal value. Its loss is dominated by reaction



and the main production pathways are the deactivation processes of  $^1\text{CH}_2$ , mainly



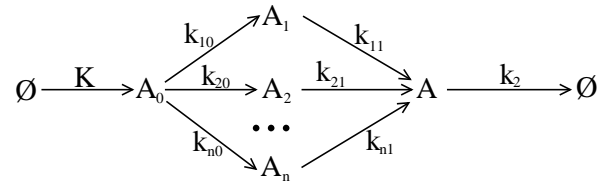
These reactions, being limited by the small concentration of  $^1\text{CH}_2$  with regard to  $\text{CH}_4$  and  $\text{H}_2$ , can be considered as pseudo-unimolecular. This system is an analog of EM 3. Having the same origin, the production pathways can be considered as a single pathway, and we recover the simple linear chain, EM 1. The uncertainty factor is thus  $F_{^3\text{CH}_2} \approx 1 + \sqrt{(F_k - 1)^2 + (F_k - 1)^2} \approx 1.14$ , to be compared with the simulation result  $F = 1.13$ .

---

**Elementary Model 3** Parallel pathways

---

**Scheme**



**Stationary solution**

Solving the system

$$\begin{aligned} \sum_{i=1}^n k_{i0} a_0 &= K \\ k_{11} a_1 &= k_{10} a_0 \\ k_{21} a_2 &= k_{20} a_0 \\ &\vdots \\ k_{n1} a_n &= k_{n0} a_0 \\ k_2 a &= \sum_{i=1}^n (k_{i1} a_i) \end{aligned}$$

one obtains

$$a = \frac{K}{k_2}$$

**Relative variance**

$$\frac{\sigma_a^2}{a^2} = \frac{\sigma_K^2}{K^2} + \frac{\sigma_{k_2}^2}{k_2^2}$$

**Notes**

As there is no flux loss or production along the chain, this model is equivalent to EM 1.

---

### 3.1.3 Other species

$C_2H$ ,  $C_2H_2$ ,  $C_2H_6$ ,  $C_2H_5$  and  $CH_3$  are involved in complex networks with loops<sup>13</sup> and bimolecular reactions and/or they are strongly correlated to each other (Fig. 1). Although we had some success with various other Elementary Models to reproduce the observed tendencies, the basic hypotheses of pathways independence and unimolecularity find here their limits. Nevertheless, uncertainty enhancement for  $C_2H$ ,  $C_2H_5$  and  $C_2H_6$  have been traced back to bimolecular effects (EM 5).

For  $C_2H_2$ , there is an equilibrium with  $C_2H$



According to EM 4, equilibrium (8) has no influence on the stationary density of  $C_2H_2$ . Moreover, this species has a loss reaction without uncertainty and 14 other production pathways, which is relevant to EM 2

$$F_{C_2H_2} \approx 1 + \sqrt{\frac{1}{14} \times 0.1^2} \approx 1.027$$

This value is larger than the simulation result ( $F = 1.01$ ), but the uncertainty attenuation is fairly well reproduced. For a better estimation, one should take explicitly into account the weak uncertainty factors of species involved in  $C_2H_2$  formation, such as  $H_2$ ,  $C_2H_4$ ,  $^1CH_2$ , etc.

### 3.1.4 Intermediate conclusion

The analysis of the 0D model shows that the relative uncertainty of many species can be explained simply by counting their direct production-loss pathways. For these species, the relative variance is inversely proportional to the number of production-loss pathways. A remarkable result, which confirms previous observations in the sensitivity analysis of such systems,<sup>12,13</sup> is that the rates of direct production pathways of these species do not contribute to the uncertainty (as in EM 2); instead, initiation processes (photodissociation) play a major role in the uncertainty budget of the whole system.

Some species are nevertheless affected by bimolecular processes, which can have various effects on the uncertainty, depending on the correlation between the reactants densities (EM 5). This correlation is determined by the overall reactions network (Fig. 1). Uncertainty enhancement is maximal for reactions between species with strongly positively correlated densities, as for instance in the formation of  $C_2H_6$  from two  $CH_3$  radicals.

## 3.2 Analysis of the 1D simulations

Considering the large prediction uncertainties observed for simulations based on evaluated reaction rates databases, it is interesting to assess the effect of reducing the uncertainty on rate coefficients to a very small value,  $F = 1.1$ , to mimic what one could expect from photochemical models when reactions rates will be measured with this kind of precision.

We compare outputs of the present simulation with the results of a state-of-the-art simulation with evaluated uncertainty factors, as presented in Hébrard *et al.*<sup>12</sup> A comparison of the mole fractions for three representative species is reported in Fig. 2 and the uncertainty

Species

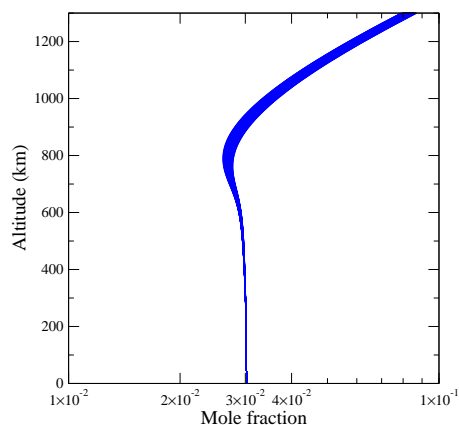
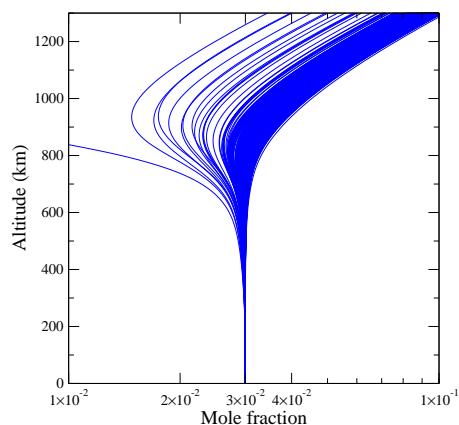
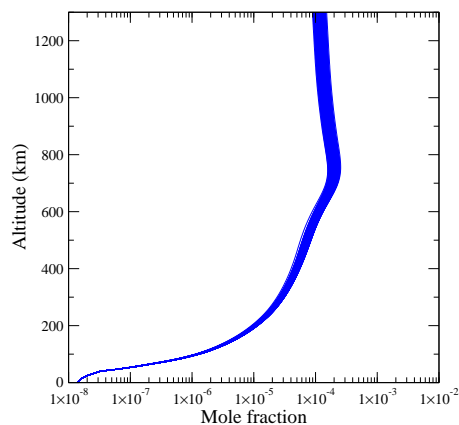
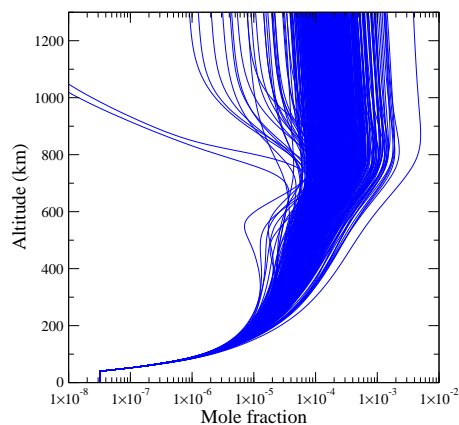
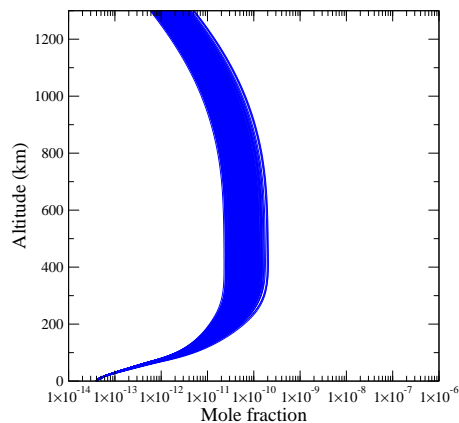
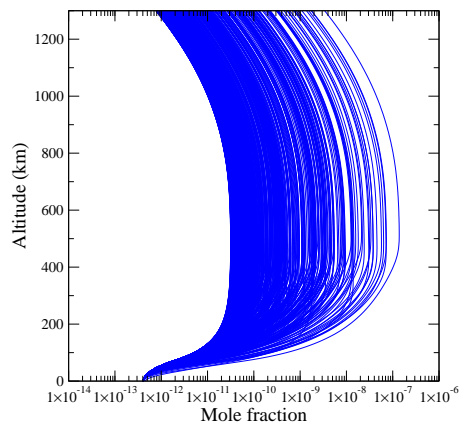
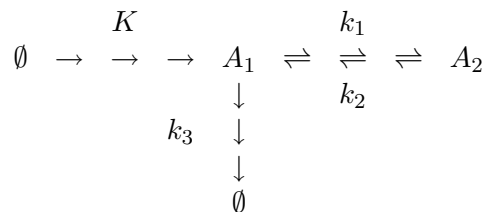
Simulation from Hébrard *et al.*<sup>12</sup>Simulation with  $F = 1.1$ CH<sub>4</sub>C<sub>2</sub>H<sub>6</sub>C<sub>6</sub>H<sub>14</sub>

Figure 2: Comparison of Monte Carlo samples of density profiles for representative hydrocarbons: (left) current *state-of-the-art* reaction rates database;<sup>12</sup> (right) simulation with all uncertainty factors set to  $F = 1.1$ . A slight shift in density at low altitudes is due to an update of boundary conditions between both simulations.

**Scheme**

**Stationary solution**

$$(k_1 + k_3) a_1 = K + k_2 a_2$$

$$k_2 a_2 = k_1 a_1$$

$$a_1 = \frac{K}{k_3}$$

**Relative variance**

$$\frac{\sigma_{a_1}^2}{a_1^2} = \frac{\sigma_K^2}{K^2} + \frac{\sigma_{k_3}^2}{k_3^2}$$

**Notes**

Another analog of EM 1.

---

factors for all species are reported for an altitude of 1200 km in Fig. 3. For  $\text{CH}_4$ , the reduction of dispersion is remarkable (the uncertainty factor  $F_{\text{CH}_4}$  at 1200 km is reduced from 1.28 to 1.02); for  $\text{C}_2\text{H}_6$ , all outlier profiles have disappeared and  $F_{\text{C}_2\text{H}_6}$  is contracted from 3.3 to 1.1; and for one of the heavier species in the model  $\text{C}_6\text{H}_{14}$ , one has a reduction of  $F_{\text{C}_6\text{H}_{14}}$  from 6.2 to 1.5, which is the largest uncertainty factor in the present  $F = 1.1$  scenario.

The uncertainty reduction for the densities of all species of the model at 1200 km is presented in Fig.3. Globally, all points lie below the curve  $F_{10\%} = F_{SA}^{0.25}$ , which means that if the density of a species had 68 % chances to lie within the interval  $[x/F_{SA}, x * F_{SA}]$ , this probability is now higher than 99.99 % (the analog on a linear scale would be for a  $1\sigma$  interval to become a  $4\sigma$  interval or better). Some species have a spectacular uncertainty reduction: for instance,  $F_{\text{C}_3\text{H}_8}$  went from 6.4 to 1.2. In the bottom left corner we observe a set of species, containing H,  $\text{H}_2$  and  $\text{CH}_4$ , having low uncertainty factors, as was also observed in the 0D model.

**3.2.1 Small species**

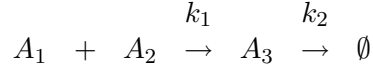
For basic species, such as H,  $\text{H}_2$ ,  $\text{CH}_4$ , or  $\text{C}_2\text{H}_4$  the results agree with the results of the 0D model (*cf.* Table 1). However, some differences are noticeable, which can be related to different factors:

- **Diffusion.** A major difference between the 0D and 1D models is transport. In these simulations, the diffusion coefficients have fixed values, which introduces in the system a production-loss process without uncertainty. When compared to 0D results, this con-

---

**Elementary Model 5** Bimolecular production

---

**Scheme****Stationary solution**

$$a_3 = \frac{k_1 a_1 a_2}{k_2}$$

**Relative variance**

In the limit where  $k_1$  has a weak influence on  $a_1$  and  $a_2$  (as in complex systems) we can assume a null correlation between these variables ( $\text{Corr}(k_1, a_1) = \text{Corr}(k_1, a_2) = 0$ ), and one gets

$$\frac{\sigma_{a_3}^2}{a_3^2} = \frac{\sigma_{k_1}^2}{k_1^2} + \frac{\sigma_{k_2}^2}{k_2^2} + \frac{\sigma_{a_1}^2}{a_1^2} + \frac{\sigma_{a_2}^2}{a_2^2} + 2\text{Corr}(a_1, a_2) \frac{\sigma_{a_1}}{a_1} \frac{\sigma_{a_2}}{a_2}$$

which involves the correlation coefficient between stationary densities  $\text{Corr}(a_1, a_2)$ , as shown in Fig. 1.

**Notes**

Depending on the correlation coefficient, the relative variance takes its values between the minimal ( $\text{Corr}(a_1, a_2) = -1$ )

$$\frac{\sigma_{a_3}^2}{a_3^2} = \frac{\sigma_{k_1}^2}{k_1^2} + \frac{\sigma_{k_2}^2}{k_2^2} + \left( \frac{\sigma_{a_1}}{a_1} - \frac{\sigma_{a_2}}{a_2} \right)^2 \geq \frac{\sigma_{k_1}^2}{k_1^2} + \frac{\sigma_{k_2}^2}{k_2^2}$$

and maximal ( $\text{Corr}(a_1, a_2) = 1$ ) value

$$\frac{\sigma_{a_3}^2}{a_3^2} = \frac{\sigma_{k_1}^2}{k_1^2} + \frac{\sigma_{k_2}^2}{k_2^2} + \left( \frac{\sigma_{a_1}}{a_1} + \frac{\sigma_{a_2}}{a_2} \right)^2$$

In the case of a dimer formation ( $A_1 = A_2$ ), the relative uncertainty corresponds to the maximal value (full positive correlation between reactants)

$$\frac{\sigma_{a_3}^2}{a_3^2} = \frac{\sigma_{k_1}^2}{k_1^2} + \frac{\sigma_{k_2}^2}{k_2^2} + 4 \frac{\sigma_{a_1}^2}{a_1^2}$$

---



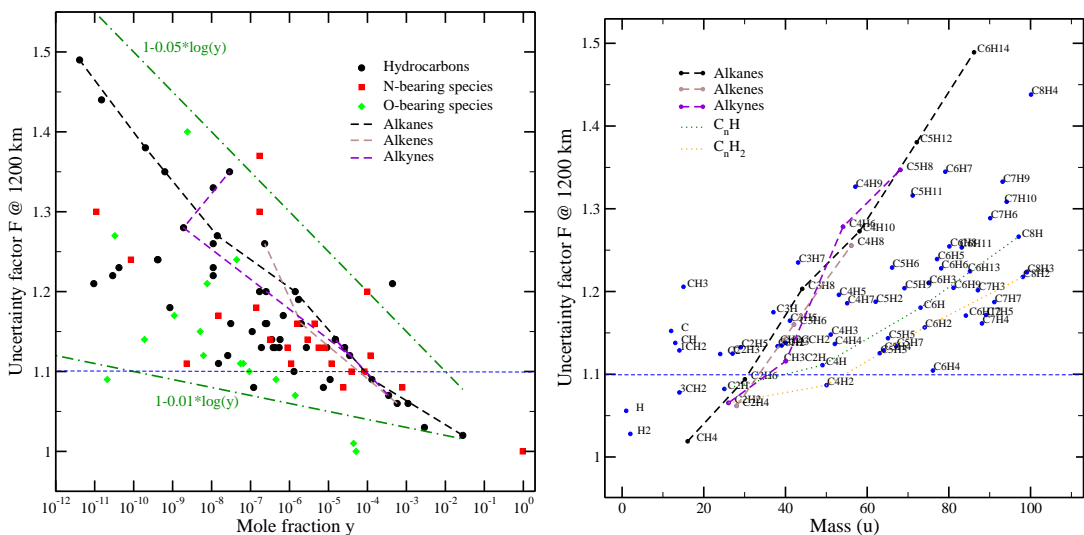


Figure 4: Correlation plots between the uncertainty factor of stationary densities at 1200 km and (left) the mole fractions, and (right) the masses. Lines are visual guides to depict some chemical families with regular pattern.

tributes to decrease globally the uncertainty on stationary densities (*cf.* Table 1), an effect which is modulated by relative values of the chemical and diffusion lifetimes for each species. The fact that we used in the 0D model a few input/output processes with fixed rates to ensure stationarity, has also an influence on the differences between the 0D and 1D results: the effect is large for those species not involved in the input/output reactions with fixed rates introduced in the 0D model, *e.g.*  $C_2H$  and  $C_2H_6$ , whereas it is very small for species such as  $H_2$ , directly concerned by these reactions.

- **Number of production and loss processes for a given species.** According to EM 2, relative uncertainty is decreased by a large number of production/loss processes. The 1D model being more complex than the 0D model, this can contribute to reduce relative uncertainty for node species as  $CH_4$ ,  $^3CH_2$ ,  $C_2H$  and  $C_2H_6$ .
- **Reactions involving reactants with very uncertain densities.** Very reactive species, such as  $C$ ,  $CH$ ,  $^1CH_2$ ,  $C_2$  and  $C_2H_3$ , can react with a lot of heavy species having large uncertainty. This is a source of uncertainty increase, when compared with less reactive species, such as  $^3CH_2$  et  $C_2H$ . Moreover,  $CH_3$  et  $C_2H_5$  are the main products of complex species metathesis, and they also suffer from larger uncertainty factors.

### 3.2.2 Uncertainty patterns for chemical families

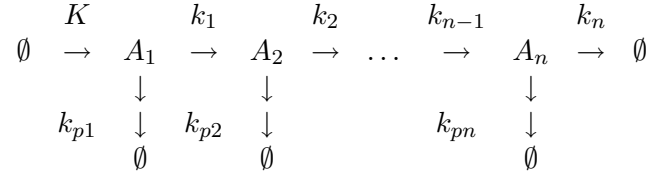
To apprehend the pattern of uncertainty distribution amongst the species, notably amongst hydrocarbons, we plotted the uncertainty factor against the mole fraction (Fig.4, left). Globally, the uncertainty factors increase as the mole fractions decrease, for all compounds. Except for a few points, the values lie between the curves  $F_{min}(y) \simeq 1 - 0.01 * \log(y)$  and

---

**Elementary Model 6** Branching chain
 

---

Scheme


**Stationary solution**

$$a_i = \frac{K}{k_i} \left[ \prod_{j=1}^i \frac{k_j}{k_j + k_{pj}} \right]$$

**Relative variance**

$$\begin{aligned}
 \frac{\sigma_{a_i}^2}{a_i^2} &= \frac{\sigma_K^2}{K^2} + \left( \frac{k_i}{k_i + k_{pi}} \right)^2 \frac{\sigma_{k_i}^2}{k_i^2} \\
 &+ \sum_{j=1}^{i-1} \left( \frac{k_{pj}}{k_j + k_{pj}} \right)^2 \frac{\sigma_{k_j}^2}{k_j^2} \\
 &+ \sum_{j=1}^i \left( \frac{k_{pj}}{k_j + k_{pj}} \right)^2 \frac{\sigma_{k_{pj}}^2}{k_{pj}^2}
 \end{aligned}$$

**Notes**

For identical rates and uncertainty factors for all reactions, one has a square root dependence of the relative uncertainty as a function of the position of the species of interest in the chain

$$\frac{\sigma_{a_i}}{a_i} = (F_k - 1) * \sqrt{1 + i/2}$$


---

$F_{max}(y) \simeq 1 - 0.05 * \log(y)$ , where  $y$  is the mole fraction. A similar plot of the uncertainty factor vs. the molecular mass is shown for hydrocarbons (Fig. 4, right). There is a positive correlation between uncertainty factor and molecular mass and also an increasing dispersion of uncertainty factors. We have shown through the Elementary Models that molecular complexification was not necessarily associated with uncertainty growth, notably when pseudo-unimolecular processes are dominant. A square-root law for growth can however be obtained in the case of a branching reaction chain (EM 6). The linear uncertainty growth observed for the 1D simulations is thus at least in part due to bimolecular reactions.

It is noteworthy that alkanes, alkenes and alkynes present identical quasi-linear trends. For alkanes, one has  $F(M) \simeq 1.012 + 0.007 * (M - M_{CH_4})$ , where  $M_{CH_4}$  is the molecular mass of  $CH_4$ . This provides a rule of thumbs in terms of number of carbon atoms  $F(n_C) \simeq 1.01 + 0.093 * (n_C - 1)$ , *i.e.* almost a 10% relative uncertainty increase by additional carbon atom. A similar linearity is observed for alkanes on the  $F$  vs. mole fraction plot, with  $F(y) \simeq 1 - 0.05 * \log(y/y_{CH_4})$ . The pattern is less regular for alkenes and alkynes. Other families, as for instance  $C_nH$  and  $C_nH_2$ , present also regular, albeit nonlinear, uncertainty growth pattern with mass (Fig. 4, right).

At the moment, we have no full explanation for this linearity of alkanes uncertainty factors. As molecular mass and mole fraction within the family are strongly anti-correlated,<sup>20</sup> it is not clear which one should be retained as an explanatory variable for this trend. Notwithstanding, we see that, when accounting only for reaction rates uncertainty, there are limits to the prediction precision by a photochemical model of the mole fractions of complex hydrocarbons.

### 3.2.3 Most influential reactions

The present simulations with reduced reaction rates uncertainty are assumed to probe the ultimate photochemical accuracy for a given model. Identification of key reactions is therefore not aiming at model precision improvement; instead, we use it here as a tool to detect influential reactions, *i.e.* reactions that affect the densities of many species.

Identification of key reactions is performed by analyzing input-output correlations (Table 2). The influence of a reaction is quantified by the number of species having input-output absolute rank correlation coefficients larger than 0.2 with this reaction. As in Hébrard *et al.*,<sup>12</sup> reactions with at least one score larger than 15 are reported.

Very few reactions are selected by this procedure. Unsurprisingly, photodissociation rates play a dominant role. This would confirm the patterns outlined for the 0D model, *i.e.* that many species are involved in quasi-unimolecular reaction chains. In terms of influence, the photodissociation of  $N_2$  and  $CH_4$  significantly affect about half of the 127 modeled species at high altitudes. This high score is equaled by the photolysis of  $C_6H_6$  at lower altitudes. Indeed, most photodissociation rates see their influence decrease with altitude, except for  $C_2H_2$  and  $C_6H_6$ . A plot comparing the cross sections of these processes (Fig. 5) shows that  $C_6H_6$  has a residual absorption in the 220-270 nm range, where the other absorbers have no impact. Similarly,  $C_2H_2$  absorbs weakly around 190-210 nm, where  $CH_4$  and  $C_2H_4$  have negligible cross-sections, and it is sufficiently more abundant than  $C_6H_6$  to have some influence.

Amongst the set of reactions, only one ( $CH + CH_4$ ) has a strong influence, almost at all altitudes. This reaction was identified in recent works about the bimodality in the density profiles of some species<sup>21</sup> and on the effect of low-T measurements on model predictivity.<sup>12</sup> In the latter study, it was shown that updating the rate constant of this reaction with low-T measured data<sup>22,23</sup> had the effect to get this reaction out of the list of key reactions. The

Reaction	300 km	600 km	900 km	1200 km
$\text{N}_2 + h\nu$	25	31	57	63
$\text{CH}_3 + h\nu$	37	46	46	49
$\text{CH}_4 + h\nu$	48	48	63	64
$\text{C}_2\text{H}_2 + h\nu$	27	11	-	-
$\text{C}_2\text{H}_4 + h\nu$	13	35	20	18
$\text{C}_6\text{H}_6 + h\nu$	69	63	31	32
$\text{CH} + \text{CH}_4$	17	30	45	42
$\text{C}_2\text{H} + \text{CH}_4$	26	13	-	-
$\text{C}_2\text{H} + \text{C}_2\text{H}_6$	18	12	11	11
$\text{C}_4\text{H} + \text{C}_2\text{H}_4$	-	23	16	16
$\text{CH}_3 + \text{CH}_3$	17	14	-	-
$\text{H} + \text{C}_2\text{H}_5$	14	14	15	15

Table 2: Key reactions with the number of species they influence at a set of representative altitudes. The total number of species in the model is 127. Reactions with at least one score larger than 15 are shown; scores below 10 are not reported.

rate constants of several others reactions identified here ( $\text{C}_2\text{H} + \text{CH}_4$ ,  $\text{C}_2\text{H} + \text{C}_2\text{H}_6$ ,  $\text{C}_4\text{H} + \text{C}_2\text{H}_6$ ) have also been recently updated at low-T.<sup>24–27</sup> The remaining uncertainty regarding currently the rates of these identified reactions, apart from some possible systematic effects, concerns mainly the nature of their products which has not been investigated thoroughly until now, even at room temperature. Other reactions rates, with much larger uncertainty factors, are currently more in need of improved accuracy. It is interesting to observe that, when all uncertainty factors are fictitiously set to a minimum achievable value,  $\text{CH} + \text{CH}_4$  and these other reactions, though to a somewhat lower extent, stand out as cornerstones of Titan’s photochemistry. Many of both experimental and theoretical studies have been published in order to investigate the rate constant of the three-body recombination reaction  $\text{CH}_3 + \text{CH}_3$  (see Klippenstein *et al.*<sup>28</sup> for a quite exhaustive review). As most of the three-body recombination reactions, very few of these studies have however been performed in conditions appropriate for planetary atmospheres. Most of the rate expressions available in the literature still have to be extrapolated down to the lowest temperatures encountered in outer planets atmospheres. This ever-existing scarcity reflects both laboratory limitations and the importance of this reaction in hydrocarbon combustion chemistry. Likewise, there is no direct measurement of the rate constant nor of the products channels of the reaction  $\text{H} + \text{C}_2\text{H}_5$  which occurs as a secondary process in the combustion studies of the  $\text{H} + \text{C}_2\text{H}_4$  and  $\text{H} + \text{C}_2\text{H}_6$  reactions;<sup>29</sup> information on any temperature dependence at conditions representative of Titan’s atmosphere is thus very limited.

Future photochemical models of Titan’s atmosphere would thus greatly benefit from a much closer investigation of the reactions identified here as it would help to improve significantly their predictivity.

## 4 Conclusion

Simulation of the atmospheric photochemistry of Titan by a 1D model and optimistically small uncertainty of reaction rates ( $F = 1.1$ ), reveal interesting features for the precision of

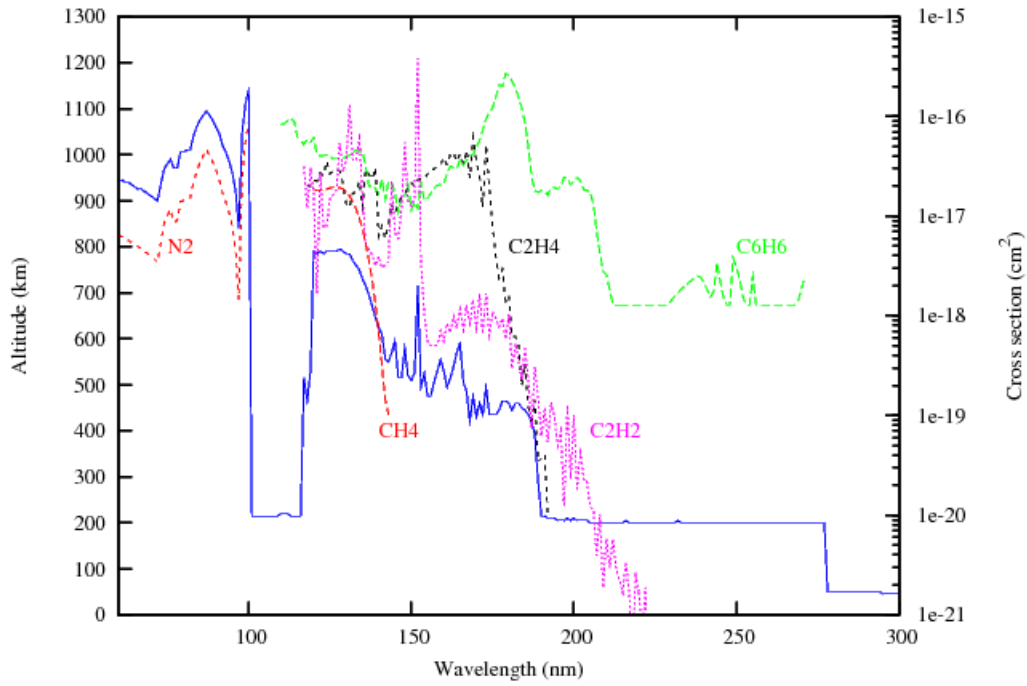


Figure 5: The depth of penetration of solar radiation as a function of wavelength in Titan's atmosphere. The blue solid line represents the altitude at which the total optical depth is unity in our 1D model. Cross sections of main absorbers are given. N<sub>2</sub> is mainly photodissociated at 1000 km, CH<sub>4</sub> at 800 km, C<sub>2</sub>H<sub>2</sub> around 600 km, C<sub>2</sub>H<sub>4</sub> around 400-500 km and C<sub>6</sub>H<sub>6</sub> around 200 km.

predicted density profiles. It has to be noted that these values correspond to a lower limit, as uncertainty sources other than chemical rates, such as diffusion coefficients, temperature, thermodynamics... have not been taken into account.

On the positive side, all modeled species densities have uncertainty factors below  $F = 1.5$ , which is a huge improvement in comparison to the present state of affairs. On a more pessimistic side, we have observed a linear increase of  $F$  with molecular mass of about 10 % per additional carbon atom for the three major hydrocarbon families. This questions the possibility to achieve predictive detailed models of molecular complexification for these species. Other chemical families present milder uncertainty increase with mass. We have still to elucidate the origins of these regular patterns in terms of reactions network structure.

Keeping in mind that the present model, as all photochemical models of Titan’s atmosphere, is not complete, the present simulations help to define limits to the predictivity/interpretation level of such models. To be deemed significant, any relative variation of the mole fraction of a compound should be larger than the relative uncertainty due to photochemistry. For a given species, let’s say  $C_3H_8$  ( $F \simeq 1.2$ ), a photochemical model would therefore not enable us to identify the origin of temporal/latitudinal/longitudinal mole fraction variations smaller than 20 %. Similarly, an additional process introduced in the model should induce a change in mole fraction of  $C_3H_8$  larger than 20 % to be considered as important for this species. This statistical concept has been used by Carrasco *et al.*<sup>19</sup> to reduce the ion-molecule reaction set for Titan’s ionosphere.

An interesting outcome of this study is that the initial processes (*e.g.* photodissociation) are always important into unimolecular reaction chains; intermediate reactions leading to a product can often be neglected, meaning that they play no role in the stationary concentration of species further in the chain. This sheds some light on the key role of photodissociations revealed by previous sensitivity analysis of this system, in apparent contradiction with the fact that photodissociation rates have modest uncertainty factors (typically estimated to  $F = 1.5$ ) when compared to many neutral-neutral reaction rates.<sup>12</sup> Of course, Titan’s atmospheric chemistry cannot be reduced to a unimolecular reactions network, and bimolecular reactions play a major role on the observed uncertainty factors of a number of species. It is difficult to predict the amplitude of their effect, because it depends strongly on the level of correlation between the reactants densities. A consequence is that it is practically impossible to ascertain beforehand the effect of the addition of new reactions into the model on the uncertainty factors of most species densities. Uncertainty propagation remains a necessary tool to solve this kind of question.

Sensitivity analysis enabled us to identify a list of reactions (Table 2), which comes as a complement to the list previously published by Hébrard *et al.*<sup>12</sup> The latter list defines *key reactions*, for which a more accurate estimation of low-T rate constants and branching ratios would impact significantly the precision of predictions with the present photochemical models; we would assign them highest priority for the improvement of model predictivity. The new list highlights a core of *influential reactions*, which would appear ultimately as key reactions (*i.e.* when all the reaction rates will be known at low-T with a precision better than 10 % and if the reaction network does not undergo drastic modifications). From our precision-oriented point of view, these reactions are of lower priority, but the accurate determination of their low-T rate constants and branching ratios is nevertheless a safe investment for the future of Titan’s photochemical modeling.

## Acknowledgments

ZP thanks the Laboratoire de Chimie Physique for financial support during his master's thesis.

## References

- [1] R. S. Stolarski, D. M. Butler and R. D. Rundel, *J. Geophys. Res.*, 1978, **83**, 3074–3078.
- [2] A. Thompson and R. Stewart, *J. Geophys. Res.*, 1991, **96**, 13089–13108.
- [3] R. Stewart and A. Thompson, *J. Geophys. Res.*, 1996, **101**, 20935–20964.
- [4] M. Dobrijevic and J. Parisot, *Planetary and Space Science*, 1998, **46**, 491–505.
- [5] N. S. Smith and F. Raulin, *Journal of Geophysical Research, [Planets]*, 1999, **104**, 1873–1876.
- [6] M. Dobrijevic, J. Ollivier, F. Billebaud, J. Brillet and J. Parisot, *A & A*, 2003, **398**, 335–344.
- [7] E. Hébrard, Y. Bénilan and F. Raulin, *Adv. Space Res.*, 2005, **36**, 268–273.
- [8] G. P. Smith and D. Nash, *Icarus*, 2005, **182**, 181–201.
- [9] E. Hébrard, M. Dobrijevic, Y. Bénilan and F. Raulin, *Planetary and Space Science*, 2007, **55**, 1470–1489.
- [10] H. Sabbah, L. Biennier, I. R. Sims, Y. Georgievskii, S. J. Klippenstein and I. W. M. Smith, *Science*, 2007, **317**, 102–105.
- [11] I. W. M. Smith, *Chemical Society Reviews*, 2008, **37**, 812–826.
- [12] E. Hébrard, P. Pernot, M. Dobrijevic, N. Carrasco, A. Bergeat, K. M. Hickson, A. Canosa, S. D. L. Picard and I. R. Sims, *J. Phys. Chem. A*, 2009, **113**, 11227–11237.
- [13] M. Dobrijevic, E. Hébrard, S. Plessis, N. Carrasco, M. Bruno-Claeys and P. Pernot, *Adv. Space Res.*, 2010, **45**, 77–91.
- [14] M. Dobrijevic, N. Carrasco, E. Hébrard and P. Pernot, *Planetary and Space Science*, 2008, **56**, 1630–1643.
- [15] J. Tellinghuisen, *Journal of Physical Chemistry A*, 2001, **105**, 3917–3921.
- [16] E. Hébrard, M. Dobrijevic, Y. Bénilan and F. Raulin, *Journal of Photochemistry and Photobiology A: Chemistry*, 2006, **7**, 211–230.
- [17] A. Saltelli, M. Ratto, S. Tarantola and F. Campolongo, *Chem. Rev.*, 2005, **105**, 2811–2827.
- [18] J. C. Helton, J. D. Johnson, C. J. Sallabery and C. B. Storlie, *Reliab. Eng. Syst. Safe.*, 2006, **91**, 1175–1209.

- [19] N. Carrasco, S. Plessis, M. Dobrijevic and P. Pernot, *International Journal of Chemical Kinetics*, 2008, **40**, 699–709.
- [20] M. Dobrijevic and I. Dutour, *Planetary and Space Science*, 2006, **54**, 287 – 295.
- [21] M. Dobrijevic, N. Carrasco, E. Hébrard and P. Pernot, *Planetary and Space Science*, 2008, **56**, 1630–1643.
- [22] A. Canosa, I. R. Sims, D. Travers, I. W. M. Smith and B. R. Rowe, *Astronomy and Astrophysics*, 1997, **323**, 644–651.
- [23] N. Daugey, P. Caubet, B. Retail, M. Costes, A. Bergeat and G. Dorthe, *Physical Chemistry Chemical Physics*, 2005, **7**, 2921–2927.
- [24] B. J. Opansky and S. R. Leone, *J. Phys. Chem.*, 1996, **100**, 19904–19910.
- [25] B. J. Opansky and S. R. Leone, *J. Phys. Chem.*, 1996, **100**, 4888–4892.
- [26] J. E. Murphy, A. B. Vakhtin and S. R. Leone, *Icarus*, 2003, **163**, 175–181.
- [27] C. Berteloite, S. D. Le Picard, P. Birza, M.-C. Gazeau, A. Canosa, Y. Bénilan and I. R. Sims, *Icarus*, 2008, **194**, 746–757.
- [28] S. Klippenstein, Y. Georgievskii and L. Harding, *Phys. Chem. Chem. Phys.*, 2006, **8**, 1133–1147.
- [29] D. L. Baulch, C. T. Bowman, C. J. Cobos, R. A. Cox, T. Just, J. A. Kerr, M. J. Pilling, D. Stocker, J. Troe, W. Tsang, R. W. Walker and J. Warnatz, *J. Phys. Chem. Ref. Data*, 2005, **34**, 757–1397.